Chinese Chemical Letters 34 (2023) 108355

Contents lists available at ScienceDirect

Chinese Chemical Letters

journal homepage: www.elsevier.com/locate/cclet

Highly active artificial potassium channels having record-high K^+/Na^+ selectivity of 20.1☆

Haowen Ma[a,b], Ruijuan Ye[c,d], Lei Jin[b], Shaoyuan Zhou[e], Changliang Ren[c,d], Haisheng Ren[e], Jie Shen[a,*], Huaqiang Zeng[a,*]

[a] College of Chemistry, Fuzhou University, Fuzhou 350116, China
[b] School of Chemistry and Chemical Engineering, Northwestern Polytechnical University, Xi'an 710072, China
[c] School of Pharmaceutical Sciences, Xiamen University, Xiamen 361102, China
[d] Shenzhen Research Institute, Xiamen University, Shenzhen 518000, China
[e] College of Chemical Engineering, Sichuan University, Chengdu 610065, China

ARTICLE INFO

Article history:
Received 21 August 2022
Revised 14 March 2023
Accepted 20 March 2023
Available online 1 June 2023

Keywords:
Supramolecular chemistry
Artificial membrane transporters
Artificial potassium channels
Crown ethers
Social self-sorting
Transport selectivity

ABSTRACT

Replicating extraordinarily high membrane transport selectivity of protein channels in artificial channel is a challenging task. In this work, we demonstrate that a strategic application of steric code-based social self-sorting offers a novel means to enhance ion transport selectivities of artificial ion channels, alongside with boosted ion transport activities. More specifically, two types of mutually compatible sterically bulky groups (benzo-crown ether and *tert*–butyl group) were appended onto a monopeptide-based scaffold, which can order the bulky groups onto the same side of a one-dimensionally aligned H-bonded structure. Strong steric repulsions among the same type of bulky groups (either benzo-crown ethers or *tert*–butyl groups), which are forced into proximity by H-bonds, favor the formation of hetero-oligomeric ensembles that carry an alternative arrangement of sterically compatible benzo-crown ethers and *tert*–butyl groups, rather than homo-oligomeric ensembles containing a single type of either benzo-crown ethers or *tert*–butyl groups. Coupled with side chain tuning, this social self-sorting strategy delivers highly active hetero-oligomeric K^+-selective ion channel $(5F12{\cdot}BF12)_n$, displaying the highest K^+/Na^+ selectivity of 20.1 among artificial potassium channels and an excellent EC_{50} value of 0.50 μmol/L (0.62 mol% relative to lipids) in terms of single channel concentration

Evolutionarily selected protein channels are often characterized by extraordinarily high selectivity in conducting molecular transport across cellular membrane. One prominent example is a family of water channel proteins called aquaporins, transporting water molecules at rate of 10^9 molecules per second while rejecting both ions and protons [1–3]. Other remarkable examples include potassium channel KcsA [4], exhibiting stunningly high K^+/Na^+ selectivity of 10^4, and proton channel M2 [5], which is $>10^5$-fold more permeable to protons than to other monovalent cations.

Serving as a rich source for biomimetic chemistry, these natural channel systems further set a high standard in membrane transport performance extremely challenging for manmade channel systems to reach. In fact, despite tremendous developments over the past four decades in artificial channel [6–15], to our best knowledge, there is only one artificial channel system that truly imitates its natural counterparts, *i.e.*, aquaporins, in terms of high water transport selectivity (high rejection of both salts and protons) while surpassing them by 150% in water transport rate [16]. Recently, significant advances also have been made in artificial proton channel [17,18], culminating in high selectivity factors of 167.6, 122.7 and 81.5 over Cl^-, Na^+ and K^+ ions, respectively, and a proton transport rate 1.22 times that of gramicidin A [18]. Other than these rare cases, efforts to replicate high selectivity seen in nature have not been very successful in developing artificial channels toward selective transport of K^+ [19–25], Na^+ [26–28], Cl^- [29–36], ClO_4^- [37] and I^- [38–40]. Particularly, while we are not aware of any Na^+-selective channel that can achieve Na^+/K^+ selectivity of >10 obtained on the basis of single channel current traces, impressive progresses in recent years have led to artificial K^+-channels that not only transport K^+ ions at ultrafast rates (Table S1 in Supporting information) but also exhibit K^+/Na^+ selectivity factors of 9.8 in 2017 [20], 14.0 [22] and 16.3 [23] in 2020, and 18.2 [24] and up to 18.9 [25] in 2021. Nevertheless, compared to KcsA's extraordinarily high K^+/Na^+ selectivity, these very modest numbers of

☆ Dedication to Prof. Lixin Dai on the Occasion of His Centenary Birthday.

* Corresponding authors.
E-mail addresses: shenjie@fzu.edu.cn (J. Shen), hqzeng@fzu.edu.cn (H. Zeng).

https://doi.org/10.1016/j.cclet.2023.108355
1001-8417/

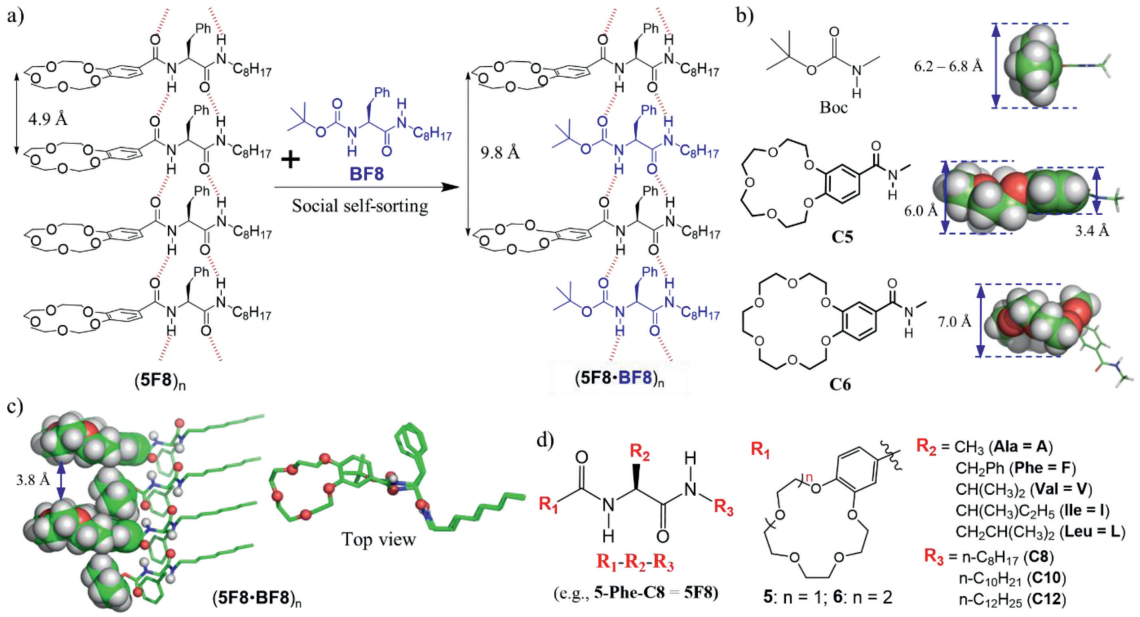

Fig. 1. (a) Self-assembled homo-oligomeric 1D structures $(5F8)_n$ might undergo a structural transformation to form heteromeric structures $(5F8{\cdot}BF8)_n$ *via* a social self-sorting process. (b) Computationally determined molecular heights of *tert*–butyl group in Boc, benzo-15-crown-5 in C5, and 18-crown-6 in C6. (c) Computationally obtained near-perfect compatibility in geometry between benzo-15-crown-5 in 5F8 and *tert*–butyl group in BF8 in the hetero-ensemble $(5F8{\cdot}BF8)_n$, having perfectly superimposable crown ether units. (d) Molecular design for combinatorial discovery of channel molecules that can pair with BF8 to produce heteromeric ensembles with enhanced ion transport activity and selectivity.

<20 certainly point to a great room of improvement for artificial channel systems.

In this article, we show that pairing crown ethers with mutually compatible *tert*–butyl groups *via* a social self-sorting process efficiently generates heteromeric channels that line up crown ethers and *tert*–butyl groups alternatively on the same side, rather than homomeric ones consisting of either crown ethers or *tert*–butyl groups. This alternative arrangement greatly alleviates the steric repulsions that otherwise exist among the vertically aligned crown ethers or *tert*–butyl groups in their homomeric channels. Significantly, the resultant heteromeric channels consistently exhibit better ion transport activities and higher K^+/Na^+ selectivities than the corresponding homomeric channels that contain only vertically arrayed crown ethers. We further found that a small change in lipophilic aliphatic side chain of the channel molecule drastically boosts its K^+/Na^+ selectivity. As such, we demonstrate that high K^+/Na^+ selectivity of 16.0 can be attained through side chain tuning, and this high selectivity can be further augmented quite substantially *via* social self-sorting to 20.1, a value that is the 5F8 (Fig. 1a) was recently demonstrated to function as an excellent K^+-selective channel, with K^+/Na^+ selectivity of 9.8 determined using single channel conduction measurement [20] and an EC_{50} (K^+) value of 6.2 μmol/L determined at the liposome level. Presumably, molecules of 5F8 with built-in H-bond functionalities self-assemble *via* intermolecular H-bonds into one-dimensional structures $(5F8)_n$, aligning appended 15-crown-5 units into an ordered array to create a transmembrane pathway for transporting K^+ ions (Fig. 1a). Formation of such H-bonded 1D structures can be supported by the crystal structures of related molecules (*e.g.*, Fmoc-Phe-C4 [41]) and many other structurally similar molecules that are able to form fibers and gel oils with high ability [42–45].

Consistent with an inter-chain separation distance of 5.0 Å seen in $(Fmoc\text{-}Phe\text{-}C4)_n$ [41], such distance in $(5F8)_n$ was computationally determined to be 4.9 Å using the COMPASS force field [46]. This value, however, is significantly smaller than the molecular height of 6.0 Å computationally determined at the B3LYP/6–31G* level for 15-crown-5 group from C5 (Fig. 1b), indicating a certain degree of conformational derivation in the crown ethers found in $(5F8)_n$ from that in C5. Computationally, this expected conformational deviation turns out to be quite significant (Fig. S1a *vs.* Fig. S1b in Supporting information), and every 15-crown-5 unit in $(5F8)_n$ was calculated to destabilize the H-bonded ensemble $(5F8)_n$ by 3.03 kcal/mol with chloroform as the explicit solvent.

To minimize the extent of structural crowdedness involving crown ethers in homo-ensemble $(5F8)_n$, one likely effective way is to introduce a steric code [47–49] to promote social self-sorting [50–52] in a way that hetero-ensemble $(5F8{\cdot}BF8)_n$ (Fig. 1a) highest among all hitherto reported artificial potassium channels and transporters [19–25,53–56] with a larger inter-chain separation distance of 9.8 Å can be formed to measurable or desirably dominant extents with respect to $(5F8)_n$ and $(BF8)_n$. We envisioned that a steric code comprising a *tert*–butyl group in Boc and a benzo-15-crown-5 unit in C5 (Fig. 1b) might help achieve desired social self-soring among molecules of Boc-containing BF8 and C5-containing 5F8, leading to preferential formation of hetero-ensemble $(5F8{\cdot}BF8)_n$ (Figs. 1a and c). This is possible since the *tert*–butyl group, having a molecular height of 6.2–6.8 Å (Fig. 1b and Fig. S1d in Supporting information), must destabilize homo-ensemble $(BF8)_n$, and thus should favor an alternative alignment with a benzene group of 3.4 Å in thickness (Figs. 1a-c). The latter arrangement generates hetero-ensemble $(5F8{\cdot}BF8)_n$ with average molecular heights of 4.8–5.1 Å involving the *tert*–butyl and benzene groups, which are compatible with the inter-chain distance of 4.9 Å. Further, upon forming $(5F8{\cdot}BF8)_n$, the separation distance between the two adjacent crown ethers increases from 4.9 Å to 9.8 Å (Fig. 1c), thereby eliminating the molecular crowdedness among crown ether units and allowing them to adopt the energetically favored conformation like that in C5. Indeed, in sharp contrast to $(5F8)_n$, the conformation of crown ether units in $(5F8{\cdot}BF8)_n$ is now found to be near-identical to that in C5 (Fig. S1a *vs.* Fig. S1c in Supporting information). Similar analysis also holds true for 6F8, containing an 18-crown-6 unit of 7.0 Å in molecular height (Fig. 1b). Consequently, mixing 6F8 with BF8 also should form hetero-ensemble $(6F8{\cdot}BF8)_n$ to good extents. This concept can

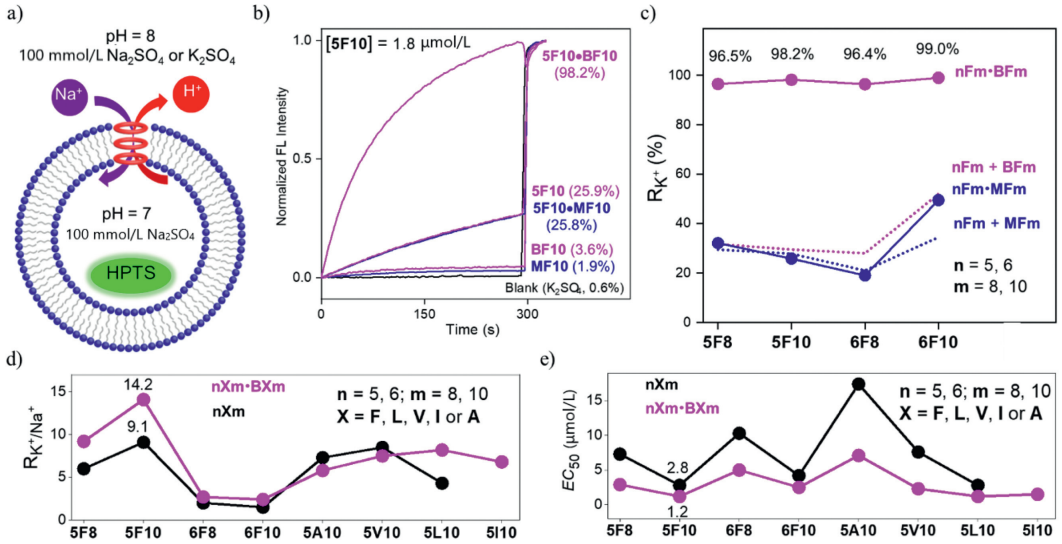

Fig. 2. (a) LUV-based HPTS assay for evaluating ion transport properties of ion channels. (b) Typical K^+ transport curves observed for hetero- and homo-ensembles such as those involving 5F10, BF10 and MF10 at 1.8 μmol/L. (c) Comparative K^+ transport efficiencies (R_{K^+}) between hetero-ensembles ($(nFm{\cdot}BFm)_n$ and $(nFm{\cdot}MFm)_n$) and homo-ensembles ($(nFm)_n$, $(BFm)_n$ and $(MFm)_n$ ($n = 5$, 6, $m = 8$, 10). (d, e) Comparative values of R_{K^+} and EC_{50} between $(nXm{\cdot}BXm)_n$ and $(nXm)_n$ where $n = 5$, 6, $m = 8$, 10, X = F, L, V, I or A. HPTS = 8-Hydroxypyrene-1,3,6-trisulfonic acid.

be additionally generalized to include non-octyl side chains of different lengths (*e.g.*, $(5Fm{\cdot}BFm)_n$ or $(6Fm{\cdot}BFm)_n$, where $m = 10$, 12, *etc.*). With this hypothetic social self-sorting-mediated formation of $(5Fm{\cdot}BFm)_n$ or $(6Fm{\cdot}BFm)_n$ ($m = 8$, 10, 12, *etc.*) using mutually compatible bulky *tert*–butyl and benzo-crown ether (*e.g.*, benzo-15-crown-5 or benzo-18-crown-6) groups, we further hypothesized that hetero-ensembles such as $(5Fm{\cdot}BFm)_n$ with an enlarged separation distance among crown ethers might differ from homo-ensembles such as $(5Fm)_n$ in terms of ion transport activity and selectivity.

In our early report [20], 5F8 and 5F10 were identified among 15 channel molecules to be the most selective and the most active K^+ transporters, respectively. In our initial screening, we therefore used these two channel molecules to pair with BF8 and BF10 to examine the above hypothesis. MF8 and MF10, both having a methyl rather than a bulky Boc group at R_1 position, are used to compare with BF8 and BF10.

Following the established protocols (Figs. 2a-c) [20,57], a pH-sensitive HPTS (8-hydroxypyrene-1,3,6-trisulfonic acid) assay was carried out to investigate the potassium transport activities of eight hetero-ensembles ($(5Fm{\cdot}BFm)_n$, $(6Fm{\cdot}BFm)_n$, $(5Fm{\cdot}MFm)_n$ and $(6Fm{\cdot}MFm)_n$ ($m = 8$ and 10)) and eight homo-ensembles ($(5Fm)_n$, $(6Fm)_n$, $(BFm)_n$ and $(MFm)_n$ ($m = 8$ and 10)). To evaluate their potassium transport activities, large unilamellar vesicles (LUVs), containing HPTS (100 μmol/L) and Na_2SO_4 (100 mmol/L) at pH 7.0, was diluted into a buffer, containing 100 mmol/L K_2SO_4 at pH 8.0, to generate a pH gradient and ion gradients (Na^+ and K^+) across LUVs. Upon addition of channel molecules, changes in fluorescence intensity of HPTS were monitored over duration of 5 min after which time triton was added to lysate the liposomes. For sodium transport study, the extravesicular K_2SO_4 was changed to Na_2SO_4.

Among four channel molecules (5F8, 5F10, 6F8 and 6F10), 5F10 produces the most active hetero-ensemble $(5F10{\cdot}BF10)_n$, with a K^+ transport efficiency (R_{K^+}) reaching 98.5% at a very low channel concentration of 1.8 μmol/L, and the remaining three channels require relatively high concentrations of 5.0, 9.0 and 4.0 μmol/L to generate similarly active hetero-ensembles with BFm (96.5%, 96.4% and 99.0%, respectively, Figs. 2b and c, Fig. S2 in Supporting information). These R_{K^+} values are much higher than the sums of R_{K^+} values from the two respective homo-ensembles (*e.g.*, 31.7%, 29.5%, 52.0% and 57.1% for $(5F8)_n+(BF8)_n$, $(5F10)_n+(BF10)_n$, $(6F8)_n+(BF8)_n$ and $(6F10)_n+(BF10)_n$, respectively) at the same concentrations. The highest enhancement by 2.3-fold was observed for 5F10 (98.5% for $(5F10{\cdot}BF10)_n$ *vs.* 29.5% for $(5F10)_n+(BF10)_n$). For comparison, for ensembles involving MFm ($m = 8$ and 10) that contains a methyl group at R_1 position, not only no significant differences were seen between homo- and hetero-ensembles, but also all ensembles exhibit low K^+ transport activities of 25.8%–58.5% (Fig. 2c and Fig. S2).

Having verified the above design hypothesis that a pair of mutually compatible bulkier Boc and benzo-crown ether groups indeed leads to substantially enhanced potassium transport activities, we subsequently looked into and compared the EC_{50} values and K^+/Na^+ selectivity in fractional activity (*e.g.*, R_{K^+}/R_{Na^+}) among the homo- and hetero-ensembles ($(nFm)_n$ *vs.* $(nFm{\cdot}BFm)_n$, $n = 5$ and 6, $m = 8$ and 10). Our recent works have demonstrated reliability of using R_{K^+}/R_{Na^+} to quickly gage the relative ion selectivity across different classes of channel molecules [20,55]. However, caution needs to be taken that R_{K^+}/R_{Na^+} could only serve as a good approximation of true ion selectivity intrinsic to any channel molecule, and the best method to determine the ion selectivity is *via* the use of single channel current measurement. From data gathered in Figs. 2d and e, Figs. S3-S8 (Supporting information), 5F10 combines with BF10 to afford the most active and selective hetero-ensemble $(5F10{\cdot}BF10)_n$. In other words, compared to an EC_{50} value of 2.8 μmol/L and a R_{K^+}/R_{Na^+} value of 9.1 in fractional activity for $(5F10)_n$, the corresponding values increase by 57% and 56% to 1.2 μmol/L and 14.2, respectively, for $(5F10{\cdot}BF10)_n$. In general, hetero-ensembles containing 15-crown-5 units were found to be more selective than 18-crown-6-containing hetero-ensembles.

An inspection of four more channel molecules derived from four other types of amino acids (5X10, X = A, V, L and I, Figs. 2d and e) establishes $(5F10{\cdot}BF10)_n$, having an EC_{50} value of 1.2 μmol/L and a R_{K^+}/R_{Na^+} value of 14.2, as the best hetero-ensemble in terms of both activity and selectivity. Based on $(5F10{\cdot}BF10)_n$, the R_3 group was further varied to include straight alkyl chains of $C_{12}H_{25}$, $C_{14}H_{29}$ and $C_{16}H_{33}$, and our results show that $(5F10{\cdot}BF10)_n$ exhibits the highest potassium transport activity of 98.2% at 1.8 μmol/L and that R_{K^+} values are 59.5%, 11.3% and 0.8% for hetero-ensembles

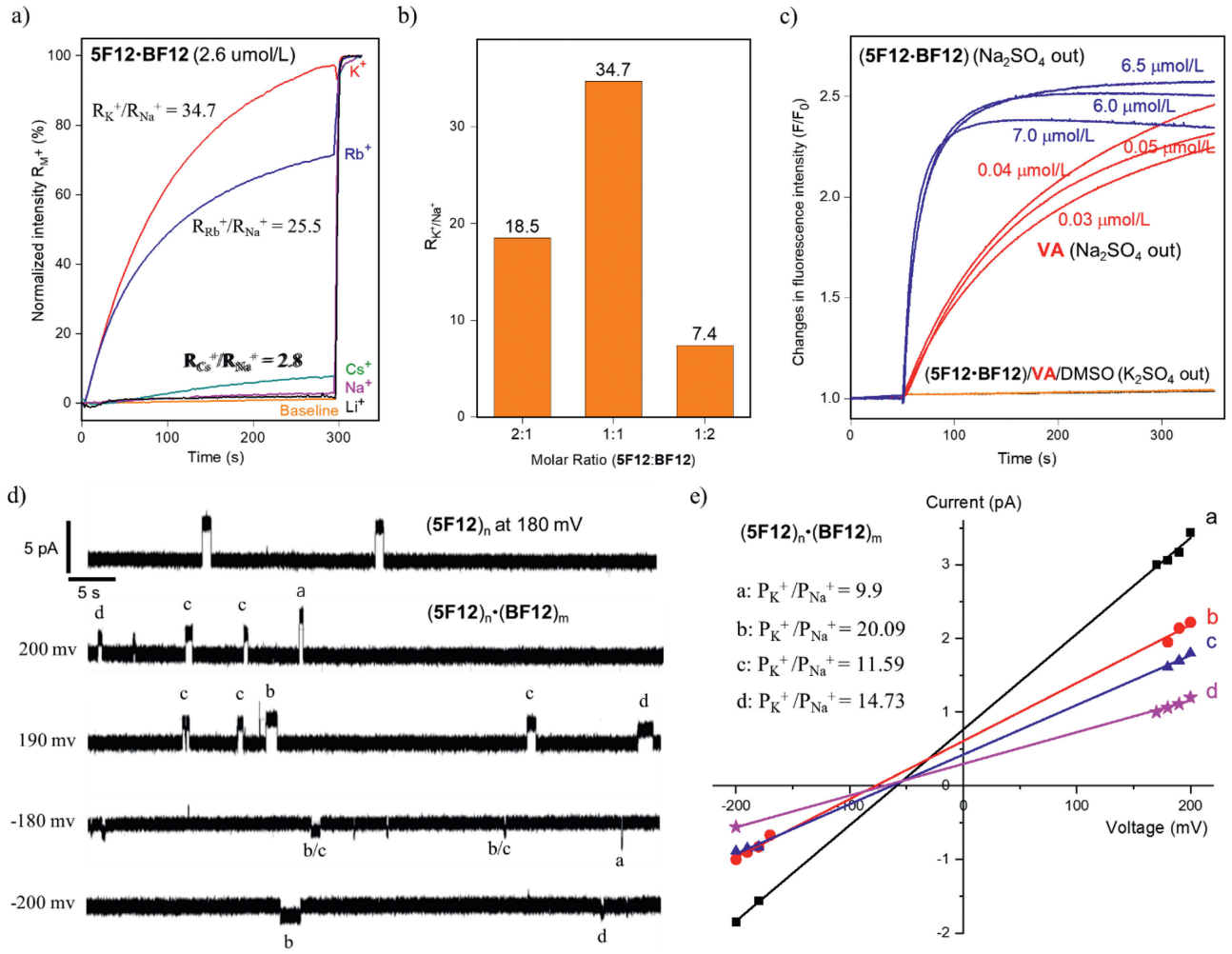

Fig. 3. (a) Ion selectivity determined for $(5F12{\cdot}BF12)_n$ at 2.6 μmol/L of 5F12. (b) Ion selectivity (R_{K^+}/R_{Na^+}) determined for $(5F12{\cdot}BF12)_n$ at total concentrations of 4.9 μmol/L for 2:1 molar ratio, 5.2 μmol/L for 1:1 molar ratio and 5.4 μmol/L for 1:2 molar ratio. (c). Changes in fluorescence intensity of Safranin O (λex = 522 nm, λem = 581 nm; 60 nmol/L) after addition of $(5F12{\cdot}BF12)_n$ from 6 μmol/L to 7 μmol/L and Valinomycin (VA) from 0.03 μmol/L to 0.05 μmol/L. The 10 mmol/L HEPES buffer at pH 7 inside LUVs contains 100 mmol/L K_2SO_4 while external HEPES buffer at pH 7 contains either 100 mmol/L K_2SO_4 or 100 mmol/L K_2SO_4. The starting background intensity F_0 at $t = 0$ was set to be 1. (d) Single channel current traces, recorded in asymmetric baths (*cis* chamber = 0.25 mol/L K_2SO_4; *trans* chamber = 0.25 mol/L Na_2SO_4), for $(5F12)_n$ and $(5F12)_n{\cdot}(BF12)_m$. (e) Determination of K^+/Na^+ selectivity for $(5F12)_n{\cdot}(BF12)_m$ that may exist in various forms at diluted concentrations using linear ohmic current-voltage (I-V) curve.

$(5F12{\cdot}BF12)_n$, $(5F14{\cdot}BF14)_n$ and $(5F16{\cdot}BF16)_n$, respectively. Nevertheless, with a slightly larger EC_{50} value of 1.5 μmol/L (Fig. S9a in Supporting information), $(5F12{\cdot}BF12)_n$ turns out to possess the highest R_{K^+}/R_{Na^+} value of 34.7 at 2.6 μmol/L (Figs. 3a). This high selectivity is followed by $(5F12)_n$, having the second highest R_{K^+}/R_{Na^+} value of 24.6 and an EC_{50} value of 2.4 μmol/L (Fig. S9b in Supporting information). In addition, deviations in 5F12:BF12 molar ratio from 1:1 drastically reduce ion selectivities of $(5F12)_{2n}{\cdot}(BF12)_n$ and $(5F12)_n{\cdot}(BF12)_{2n}$ by 47% and 79% to 18.5% and 7.4% (Fig. 3b and Fig. S10 in Supporting information), respectively. Selective ion transport could cause an asymmetrical accumulation of ions across LUVs, resulting in membrane polarization that can be probed by using voltage-sensitive Safranin O. For this experiment, LUVs, containing 100 mmol/L K_2SO_4, was diluted into a solution, containing 100 mmol/L Na_2SO_4 and 60 nmol/L Safranin O. After system equilibrium for 50 s, $(5F12{\cdot}BF12)_n$ or Valinomycin (VA, a highly selective K^+ carrier) at various concentrations were added, and changes in fluorescence intensity were monitored for 300 s with fluorescence intensity at $t = 0$ s set to be 1 (Fig. 3c). Compared to control experiments where both intra- and extravesicular salts are kept as K_2SO_4 (denoted as "K_2SO_4 out" in Fig. 3c) as well as other channel/carrier concentrations (1.25–10 μmol/L for $(5F12{\cdot}BF12)_n$ and 0.01–0.08 μmol/L for VA, Fig. S11 in Supporting information), channel $(5F12{\cdot}BF12)_n$ at 6.5 μmol/L and carrier VA at 0.5 μmmol/L induce the largest changes of 157% and 146% in fluorescence intensity of Safranin O, respectively. These comparative data establish high K^+/Na^+ selectivity in K^+ transport mediated by $(5F12{\cdot}BF12)_n$.

Membrane integrity in the absence and presence of channels $(5F12)_n$ or $(5F12{\cdot}BF12)_n$ was then evaluated using a self-quenching dye made up of a mixture of 5-carboxyfluorescein and 6-carboxyfluorescein (CF). These two CF isomers have dimensions of 9.2 × 11.4 Å and 10 Å × 10 Å (Fig. S12 in Supporting information), respectively. For this assay, CF dyes were trapped inside LUVs at a high concentration of 50 mmol/L such that they exist in mostly non-fluorescent dimer state. If channel molecules form a pore larger than 1 nm or result in membrane lysis, the leaked CF dimer molecules will largely dissociate to form more fluorescent monomers. As shown in Fig. S12, addition of $(5F12)_n$ (EC_{50} = 2.4 μmol/L) or $(5F12{\cdot}BF12)_n$ (EC_{50} = 1.5 μmol/L) at 15 μmol/L into dye-containing LUVs does not produce any noticeable changes in fluorescence intensity relative to the background signals. These results are in sharp contrast to efflux of 59% and

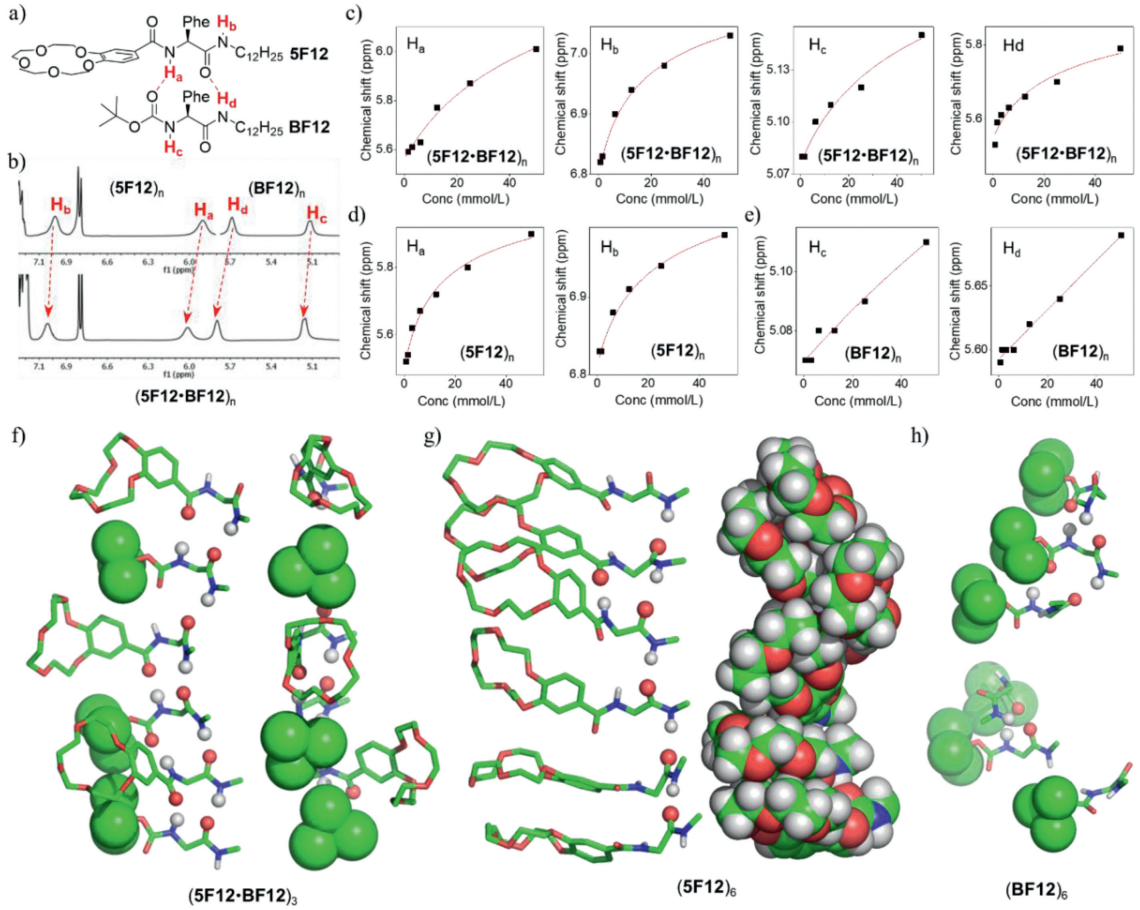

Fig. 4. (a) Structure of hetero-ensembles $(5F12·BF12)_n$. (b) Comparative partial ^1H NMR spectra of $(5F12)_n$, $(BF12)_n$ and $(5F12·BF12)_n$ at 50 mmol/L at room temperature. (c-e) Concentration-dependent changes in chemical shift for protons a-d found in $(5F12·BF12)_n$, $(5F12)_n$ and $(BF12)_n$ from 0.78 mmol/L to 50 mmol/L at room temperature. (f-h) Illustrate molecular dynamics-simulated structures of $(5F12·BF12)_3$, $(5F12)_6$ and $(BF12)_6$ in POPC membrane. Small balls in gray (H-atoms) and red (O-atoms) represent atoms that are within H-bonding distance of <2.5 Å and side chains R2 and R3 as well as non-amide H-atoms have been removed for clarity of view. POPC = 1-palmitoyl-2-oleoyl-*sn*–glycero-3-phosphocholine.

99% dye molecules caused by Melittin at 0.25 and 1 μmol/L, respectively, thereby confirming that the observed changes in fluorescence intensity of HPTS or Safranin O in the presence of channel molecules are a consequence of the selective transport of K^+ ions, rather than membrane lysis, by channel molecules.

Single channel conductance measurements were then carried out on $(5F12)_n$ and $(5F12·BF12)_n$, having the highest selectivities among all channels studied herein. The observation of a series of multiple single channel current traces, which were recorded at different voltages in unsymmetrical baths (*cis* chamber = 0.2 mol/L K_2SO_4 and *trans* chamber = 0.2 mol/L Na_2SO_4, Fig. 3d and Figs. S13-S15 in Supporting information), unambiguously confirm single channel mechanism underlying the selective K^+ transport by both $(5F12)_n$ and $(5F12·BF12)_n$. Plotting current *vs.* voltage (I-V curve, Fig. S13) gives rise to high K^+/Na^+ selectivity (P_{K^+}/P_{Na^+}) of 16.0 for $(5F12)_n$. Interestingly, for $(5F12·BF12)_n$, four sets of I-V curves (curves a-d, Fig. 3e and Fig. S14) could be identified from which P_{K^+}/P_{Na^+} values were determined to be 9.9, 20.1, 11.6 and 14.7 respectively. Coupled with the molar ratio-dependent changes in ion selectivity presented in Fig. 3b and high K^+/Na^+ selectivity of 16.0 for $(5F12)_n$, we believe a high P_{K^+}/P_{Na^+} value of 20.1 should result from $(5F12·BF12)_n$, and value of 14.7 can be assigned to channels containing more 5F12 than BF12 (*e.g.*, $(5F12)_n·(5F12·BF12)_m$ where $n \geq 1$), and both 11.6 and 9.9 likely might correspond to $(5F12·BF12)_m·(BF12)_n$ where $n \geq 1$.

Comparing changes in chemical shift of H-bond-forming protons is a well-established method for studying the association among molecules that contain H-bond donors and acceptors [58–61]. Here, an equal molar mixing of 5F12 and BF12 at 50 mmol/L produces not only well-defined ^1H NMR signals, but also noticeable downfield shifts of 0.11, 0.05, 0.04 and 0.10 ppm for protons H_a, H_b, H_c and H_d of hetero-ensemble $(5F12·BF12)_n$ relative to those found in homo-ensembles $(5F12)_n$ and $(BF12)_m$ (Figs. 4a and b). These signify the formation of $(5F12·BF12)_n$ from molecules 5F12 and BF12. Subsequent concentration-dependent ^1H NMR investigations from 0.78 mmol/L to 50 mmol/L lead to signals that can be fitted using a non-linear regression analysis method, suggesting these four protons be involved in forming defined H-bonds (Fig. 4c). But it needs to be pointed out that fitting using a simple dimerization equation to obtain association constants was not attempted since other oligomeric species may co-exist in equilibrium. Signal fitting is further complicated by the fact that formation of $(5F12·BF12)_n$ requires self-assembled $(5F12)_n$ to break first, a process that requires a very sophisticated treatment, which is beyond the scope of the current work. Interestingly, while non-linear regression analyses of protons H_a and H_b also support the formation of H-bonded homo-ensemble $(5F12)_n$ (Fig. 4d), the same analyses on protons H_c and H_d prove inability of BF12 to form well-defined self-assembled $(BF12)_n$ (Fig. 4e). As such, we believe monomer and other oligomers involving BF12 might co-exist in a poorly defined fashion. This likelihood can be corroborated by

its large size of 6.2–6.8 Å (Fig. 1b), which is much larger than the inter-chain separation distance of 4.9 Å (Fig. 1a), and further by the molecular dynamics simulation (Fig. 4h).

To obtain its possible structures in the membrane, a hybrid K^+-selective ion channel $(5F12{\cdot}BF12)_n$ was computationally optimized using the COMPASS force field [46]. The resultant structure shown in Fig. 1c was then placed in a bilayer of 128 POPC molecules (1-palmitoyl-2-oleoyl-*sn*–glycero-3-phospho choline) solvated on two sides by 2×2397 water molecules (Fig. 4a) and subjected to MD simulation. Given the hydrophobic thickness of ~28 Å for POPC bilayer [62] and an inter-chain separation distance of 4.9 Å for $(5F12{\cdot}BF12)_n$, n value was set to be 3 for MD simulation. After equilibration steps, the production run was carried out for 20 ns. Similar simulation steps were also performed on homo-ensembles $(5F12)_6$ and $(BF12)_6$. Highly populated and representative structures seen in the last 5 ns trajectories for $(5F12{\cdot}BF12)_3$, $(5F12)_6$ and $(BF12)_6$ were presented in Figs. 4f-h.

Structural analyses of these MD-simulated structures pleasantly reveal features that validate our above premise in using mutually compatible bulky groups (benzene-modified crown ether and *tert*–butyl group) to promote the formation of hetero-ensembles (*e.g.*, $(5Fm{\cdot}BFm)_n$ or $(6Fm{\cdot}BFm)_n$, $m = 8$, 10, 12, *etc.*) *via* a social self-sorting process. That is, an alternative arrangement of three molecules of 5F12, containing a bulky benzo-crown ether, with three molecules of BF12, containing a bulky *tert*–butyl group, indeed leads to an H-bonded hetero-ensemble $(5F12{\cdot}BF12)_3$, possessing nine intermolecular H-bonds with a loss of one H-bond (Fig. 4f). In contrast, the bulky crown ether units in $(5F12)_6$ result in a loss of four H-bonds that are immediately adjacent to crown ethers, but appear to exert little influence on the remaining more distant five H-bonds (Fig. 4g). For $(BF12)_6$, the six bulky *tert*–butyl groups break the hexamer into three isolated species, *i.e.*, trimer, dimer and monomer (Fig. 4h), which are consistent with the NMR dilution experiment (Fig. 4e). Although some structural differences for $(5F12{\cdot}BF12)_3$ in the gas phase and in the POPC membrane can be noted (Fig. 1c *vs.* Fig. 4f), the three crown ethers are well separated from each other with ample spaces around them to mediate a faster and more selective transport of K^+ ions ($P_{K^+}/P_{Na^+} = 20.1$, $EC_{50} = 1.5$ μmol/L). On the other hand, a very crowded arrangement of six crown ethers in $(5F12)_6$ must greatly diminish the channel's ion transport activity and selectivity ($P_{K^+}/P_{Na^+} = 16.0$, $EC_{50} = 2.4$ μmol/L).

The ability to control self-assembly of two or more components is crucial in creating smart peptide biomaterials. With solid and consistent evidence, we have demonstrated here the steric code-mediated social self-sorting as an effective strategy for enhancing both ion transport activities and selectivities of K^+-selective ion channels. In the first round of screening that focuses on eight K^+-selective channels containing C_8H_{17} or $C_{10}H_{21}$ side chains, this strategy achieves both substantial enhancements in K^+ transport activity by 68% to 230% for all channels and significant increases in K^+/Na^+ selectivity, particularly for phenylalanine-based channels. From this screening, hetero-ensemble $(5F10{\cdot}BF10)_n$ emerge as the best channels in terms of both ion transport activity and selectivity. On this basis, the subsequent screening using the same strategy, which is in further combination with the side chain tuning, culminated in the discovery of highly sought-after hetero-oligomeric K^+ channel $(5F12{\cdot}BF12)_n$. While the HPTS-based assay gives rise to an excellent K^+ transport activity ($EC_{50} = 1.5$ μmol/L = 1.8 mol% relative to lipids, or 0.5 μmol/L, 0.62 mol% in terms of single channel concentration) for $(5F12{\cdot}BF12)_n$ with n likely equal to 3 in the lipid membrane, single channel current measurements yield the highest K^+/Na^+ selectivity ($P_{K^+}/P_{Na^+} = 20.1$) among all hitherto reported K^+-selective channels.

Declaration of competing interest

The authors declare that they have no known competing financial interests or personal relationships that could have appeared to influence the work reported in this paper.

Acknowledgments

This work was supported by the National Natural Science Foundation of China (No. 22271049), Fuzhou University, Xiamen University and Northwestern Polytechnical University.

Supplementary materials

Supplementary material associated with this article can be found, in the online version, at doi:10.1016/j.cclet.2023.108355.

References

[1] P. Agre, Proc. Am. Thoracic Soc. 3 (2006) 5–13.
[2] K. Murata, K. Mitsuoka, T. Hirai, et al., Nature 407 (2000) 599–605.
[3] E. Tajkhorshid, P. Nollert, M.Ø. Jensen, et al., Science 296 (2002) 525–530.
[4] D.A. Doyle, J.Morais Cabral, R.A. Pfuetzner, et al., Science 280 (1998) 69–77.
[5] J.A. Mould, H.C. Li, C.S. Dudlak, et al., J. Biol. Chem. 275 (2000) 8592–8599.
[6] A. Vargas Jentzsch, A. Hennig, J. Mareda, S. Matile, Acc. Chem. Res. 46 (2013) 2791–2800.
[7] J. Montenegro, M.R. Ghadiri, J.R. Granja, Acc. Chem. Res. 46 (2013) 2955–2965.
[8] T.M. Fyles, Acc. Chem. Res. 46 (2013) 2847–2855.
[9] F. Otis, M. Auger, N. Voyer, Acc. Chem. Res. 46 (2013) 2934–2943.
[10] G.W. Gokel, S. Negin, Acc. Chem. Res. 46 (2013) 2824–2833.
[11] Y. Zhao, H. Cho, L. Widanapathirana, S. Zhang, Acc. Chem. Res. 46 (2013) 2763–2772.
[12] B. Gong, Z. Shao, Acc. Chem. Res. 46 (2013) 2856–2866.
[13] Y.P. Huo, H.Q. Zeng, Acc. Chem. Res. 49 (2016) 922–930.
[14] J.Y. Chen, J.L. Hou, Org. Chem. Front. 5 (2018) 1728–1736.
[15] S.P. Zheng, L.B. Huang, Z. Sun, M. Barboiu, Angew. Chem. Int. Ed. 60 (2021) 566–597.
[16] A. Roy, J. Shen, H. Joshi, et al., Nat. Nanotech. 16 (2021) 911–917.
[17] T. Yan, S. Liu, J. Xu, H. Sun, S. Yu, J. Liu, Nano Lett. 21 (2021) 10462–10468.
[18] J. Shen, R.J. Ye, Z. Liu, H.Q. Zeng, Angew. Chem. Int. Ed. 61 (2022) e202200259.
[19] C. Lang, X. Deng, F. Yang, et al., Angew. Chem. Int. Ed. 129 (2017) 12842–12845.
[20] C.L. Ren, J. Shen, H.Q. Zeng, J. Am. Chem. Soc. 139 (2017) 12338–12341.
[21] M. Barboiu, Acc. Chem. Res. 51 (2018) 2711–2718.
[22] L.Z. Zeng, H. Zhang, T. Wang, T. Li, Chem. Commun. 56 (2020) 1211–1214.
[23] F. Chen, J. Shen, N. Li, et al., Angew. Chem. Int. Ed. 59 (2020) 1440–1444.
[24] S. Qi, C. Zhang, H. Yu, et al., J. Am. Chem. Soc. 143 (2021) 3284–3288.
[25] D. Qiao, H. Joshi, H. Zhu, et al., J. Am. Chem. Soc. 143 (2021) 15975–15983.
[26] A. Nakano, Q. Xie, J.V. Mallen, L. Echegoyen, G.W. Gokel, J. Am. Chem. Soc. 112 (1990) 1287–1289.
[27] G.W. Gokel, A. Mukhopadhyay, Chem. Soc. Rev. 30 (2001) 274–286.
[28] F. Otis, C. Racine-Berthiaume, N. Voyer, J. Am. Chem. Soc. 133 (2011) 6481–6483.
[29] V. Gorteau, G. Bollot, J. Mareda, A. Perez-Velasco, S. Matile, J. Am. Chem. Soc. 128 (2006) 14788–14789.
[30] C.R. Yamnitz, S. Negin, I.A. Carasel, R.K. Winter, G.W. Gokel, Chem. Commun. 46 (2010) 2838–2840.
[31] A. Vargas Jentzsch, S. Matile, J. Am. Chem. Soc. 135 (2013) 5302–5303.
[32] T. Saha, A. Gautam, A. Mukherjee, M. Lahiri, P. Talukdar, J. Am. Chem. Soc. 138 (2016) 16443–16451.
[33] X. Wei, G. Zhang, Y. Shen, et al., J. Am. Chem. Soc. 138 (2016) 2749–2754.
[34] C. Ren, X. Ding, A. Roy, et al., Chem. Sci. 9 (2018) 4044–4051.
[35] C.L. Ren, F. Zeng, J. Shen, et al., J. Am. Chem. Soc. 140 (2018) 8817–8826.
[36] W.L. Huang, X.D. Wang, Y.F. Ao, Q.Q. Wang, D.X. Wang, J. Am. Chem. Soc. 142 (2020) 13273–13277.
[37] L. Yuan, P. Jiang, J. Hu, et al., Chin. Chem. Lett. 33 (2022) 2026–2030.
[38] B.P. Benke, P. Aich, Y. Kim, et al., J. Am. Chem. Soc. 139 (2017) 7432–7435.
[39] L. Yuan, J. Shen, R.J. Ye, F. Chen, H.Q. Zeng, Chem. Commun. 55 (2019) 4797–4800.
[40] A. Roy, H. Joshi, R.J. Ye, et al., Angew. Chem. Int. Ed. 59 (2020) 4806–4813.
[41] C.L. Ren, G.H.B. Ng, H. Wu, et al., Chem. Mater. 28 (2016) 4001–4008.
[42] C.L. Ren, J. Shen, F. Chen, H.Q. Zeng, Angew. Chem. Int. Ed. 56 (2017) 3847–3851.
[43] C.L. Ren, F. Chen, F. Zhou, Langmuir 32 (2016) 13510–13516.
[44] J.T. Li, Y.P. Huo, H.Q. Zeng, J. Mater. Chem. A 6 (2018) 10196–10200.
[45] J.T. Li, Y.P. Huo, H.Q. Zeng, Langmuir 34 (2018) 8058–8064.
[46] H. Sun, J. Phys. Chem. B 102 (1998) 7338–7364.
[47] B.H. Northrop, Y.R. Zheng, K.W. Chi, P.J. Stang, Acc. Chem. Res. 42 (2009) 1554–1563.
[48] M.M. Safont-Sempere, G. Fernández, F. Würthner, Chem. Rev. 111 (2011) 5784–5814.
[49] J. Shen, R. Ye, H. Zeng, Angew. Chem. Int. Ed. 60 (2021) 12924–12930.
[50] W. Jiang, C.A. Schalley, Proc. Natl. Acad. Sci. U. S. A. 106 (2009) 10425–10429.

[51] J.M. Lehn, Angew. Chem. Int. Ed. 54 (2015) 3276–3289.
[52] H. Jędrzejewska, A. Szumna, Chem. Rev. 117 (2017) 4863–4899.
[53] Z. Sun, M. Barboiu, Y.M. Legrand, E. Petit, A. Rotaru, Angew. Chem. Int. Ed. 127 (2015) 14681–14685.
[54] C. Ren, F. Chen, R.J. Ye, et al., Angew. Chem. Int. Ed. 58 (2019) 8034–8038.
[55] R.J. Ye, C.L. Ren, J. Shen, et al., J. Am. Chem. Soc. 141 (2019) 9788–9792.
[56] N. Li, F. Chen, J. Shen, et al., J. Am. Chem. Soc. 142 (2020) 21082–21090.
[57] H.Q. Zhao, S. Sheng, Y.H. Hong, H.Q. Zeng, J. Am. Chem. Soc. 136 (2014) 14270–14276.
[58] H.Q. Zeng, R.S. Miller, I. Robert A. Flowers, B. Gong, J. Am. Chem. Soc. 122 (2000) 2635–2644.
[59] H.Q. Zeng, H. Ickes, I. Robert A. Flowers, B. Gong, J. Org. Chem. 66 (2001) 3574–3583.
[60] H.Q. Zeng, X.W. Yang, I. Robert A. Flowers, B. Gong, J. Am. Chem. Soc. 124 (2002) 2903–2910.
[61] H.Q. Zeng, X. Yang, A.L. Brown, et al., Chem. Commun. 13 (2003) 1556–1557.
[62] Y. Guo, S. Pogodin, V.A. Baulin, J. Chem. Phys. 140 (2014) 174903.